Available online at www.sciencedirect.com
ScienceDirect
Journal of Hazardous Materials 154 (2008) 237–244
Journal of Hazardous Materials
www.elsevier.com/locate/jhazmat

Batch removal of malachite green from aqueous solutions by adsorption on oil palm trunk fibre: Equilibrium isotherms and kinetic studies

B.H. Hameed [a,*], M.I. El-Khaiary [b]

[a] *School of Chemical Engineering, Engineering Campus, Universiti Sains Malaysia, 14300 Nibong Tebal, Penang, Malaysia*
[b] *Chemical Engineering Department, Faculty of Engineering, Alexandria University, El-Hadara, Alexandria 21544, Egypt*

Received 6 September 2007; received in revised form 5 October 2007; accepted 5 October 2007
Available online 11 October 2007

Abstract

Oil palm trunk fibre (OPTF) – an agricultural solid waste – was used as low-cost adsorbent to remove malachite green (MG) from aqueous solutions. The operating variables studied were contact time, initial dye concentration, and solution pH. Equilibrium adsorption data were analyzed by three isotherms, namely the Freundlich isotherm, the Langmuir isotherm, and the multilayer adsorption isotherm. The best fit to the data was obtained with the multilayer adsorption. The monolayer adsorption capacity of OPTF was found to be 149.35 mg/g at 30 °C. Adsorption kinetic data were modeled using the Lagergren pseudo-first-order, Ho's pseudo-second-order and Elovich models. It was found that the Lagergren's model could be used for the prediction of the system's kinetics. The overall rate of dye uptake was found to be controlled by external mass transfer at the beginning of adsorption, then for initial MG concentrations of 25, 50, 100, 150, and 300 mg/L the rate-control changed to intraparticle diffusion at a later stage, but for initial MG concentrations 200 and 250 mg/L no evidence was found of intraparticle diffusion at any period of adsorption. It was found that with increasing the initial concentration of MG, the pore-diffusion coefficient increased while the film-diffusion coefficient decreased.

Keywords: Oil palm trunk; Malachite green; Adsorption isotherm; Equilibrium; Kinetics

1. Introduction

Synthetic dyes are extensively used in many industries such as the textile, leather tanning, paper production, food technology, hair colorings, etc. Wastewaters discharged from these industries are usually polluted by dyes. Malachite green (MG) is most commonly used for the dyeing of cotton, silk, paper, leather and also in manufacturing of paints and printing inks. Malachite green is widely used in distilleries for coloring purposes [1]. Malachite green has properties that make it difficult to remove from aqueous solutions and also toxic to major microorganisms [2]. Though the use of this dye has been banned in several countries and not approved by US Food and Drug Administration [3], it is still being used in many parts of the world due to its low-cost, ready availability and efficacy [4] and to lack of a proper alternative. Its use in the aquaculture practice in many countries, including Malaysia has not been regulated [5]. Malachite green when discharged into receiving streams will affect the aquatic life and causes detrimental effects in liver, gill, kidney, intestine, gonads and pituitary gonadotrophic cells [6]. Therefore, the treatment of effluent containing such dye is of interest due to its esthetic impacts on receiving waters.

Various attempts have been made for MG removal from the wastewater. These include photo-degradation [7,8], photocatalytic degradation [9–11] and adsorption [12,13]. Activated carbon has been widely investigated for the adsorption of basic dyes [14–18]. However, extensive research has been undertaken recently to develop alternative and economic adsorbents. A number of non-conventional sorbents has been reported in the literature for their capacity to remove malachite green from aqueous solutions, such as de-oiled soya [19], agro-industry waste, *Prosopis cineraria* [20], bagasse fly ash [21], hen feathers [22]., iron humate [23] and modified rice straw [24].

In this work, we attempt to utilize oil palm trunk fibre (OPTF), an agricultural solid waste periodically left in the field on replanting and pruning, as an alternative low-cost sorbent in the removal of malachite green from aqueous solutions. Palm-oil industry is one of the most important agro-industries in Malaysia [25]. The

* Corresponding author. Fax: +60 4 594 1013.
E-mail address: chbassim@eng.usm.my (B.H. Hameed).

0304-3894/$ – see front matter © 2007 Elsevier B.V. All rights reserved.
doi:10.1016/j.jhazmat.2007.10.017

Malaysian palm-oil industry is growing rapidly and becomes a very important agriculture-based industry, where the country today is the world's largest exporter of palm oil and expects output in 2006 to be up 5% at almost 16 M tonnes. Oil palm trunk is a major lignocellulosic-rich, solid waste material generated from palm-oil upstream industry [26]. As a result of declining yields, replanting of trees is usually carried out after 25–30 years. Lim [27] estimated that the replanting of 1 ha generates about 80.4 tonnes of dry biomass, of which palm trunks contribute about 66 tonnes and fronds 14.4 tonnes. Replanting activity is expected to increase substantially starting from this decade. Thus, large quantities of biomass, of the order of a few million tonnes of dry matter, will from now on be generated annually [28]. Trunks of mature trees that have been cut to allow replanting should be recycled more effectively. Currently most of the felled trees are sectioned and either left to rot on the plantation grounds or are piled into stacks for eventual burning [29]. When left on the plantation floor, these waste materials create great environmental problems. Therefore, economic utilization of these fibres will be beneficial.

The objective of our investigation was to investigate the potential of OPTF, an agricultural solid waste, as a novel adsorbent in the removal of the basic dye, malachite green, from aqueous solutions.

2. Materials and methods

2.1. Adsorbate

The dye, malachite green oxalate, C.I. Basic Green 4, C.I. Classification Number 42,000, chemical formula = $C_{52}H_{54}N_4O_{12}$, MW = 927.00, λ_{max} = 618 nm (measured value) was supplied by Sigma–Aldrich (M) Sdn Bhd, Malaysia and used as received. Fig. 1 shows the chemical structure of malachite green oxalate.

2.2. Adsorbent

Section of oil-palm trunk was procured from a plantation not far from the Engineering campus, Nibong Tebal. The section was left to dry naturally out site the laboratory. The dried section was firstly chopped to pieces ca 1 in.^{3} in size, ground and sieved to obtain a particle size range of 0.5–1 mm. The prepared sample was washed repeatedly with boiled water till washed water is clear from any color and finally washed with deionized water and oven dried at 70 °C for 24 h to constant weight. The dried sample was stored in plastic bottle for further use. No other chemical or physical treatments were used prior to adsorption experiments. The chemical composition of the oil palm trunk fibre (% dry weight, w/w) is the following: cellulose 41.2%, hemicelluloses 34.4%, lignin 17.1%, ash 3.4%, extractives 0.5%, and ethanol solubles 2.3% [30].

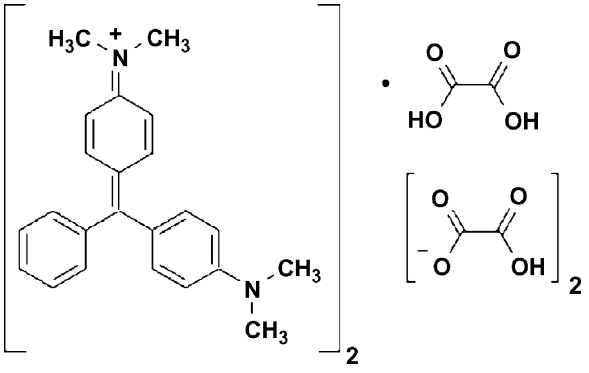

Fig. 1. Chemical structure of malachite green oxalate.

2.3. Preparation and characterization of the sorbent

The surface functional groups of the OPTF were detected by Fourier transform infrared (FTIR) spectroscope (FTIR-2000, Perkin-Elmer). The spectra were recorded from 4000 to 400 cm^{-1}. In addition, Scanning electron microscopy (SEM) analysis was carried out for the OPTF to study the surface morphology before and after MG adsorption.

2.4. Equilibrium studies

Batch equilibrium studies were carried out by adding a fixed amount of sorbent (0.30 g) into 250-mL Erlenmeyer flasks containing 200 mL of different initial concentrations (25–300 mg/L) of dye solution at pH 5. The flasks were agitated in an isothermal water-bath shaker at 130 rpm and 30 °C for 2 h until equilibrium was reached. Aqueous samples were taken from the solutions and the concentrations were analyzed. At time $t = 0$ and at equilibrium, the dye concentrations were measured by a double beam UV/vis spectrophotometer (Shimadzu, Model UV 1601, Japan) at 618 nm. The amount of equilibrium adsorption, q_e (mg/g), was calculated by:

$$q_e = (C_o - C_e)\frac{V}{W} \quad (1)$$

where C_o and C_e (mg/L) are the liquid-phase concentrations of dye at initial and equilibrium, respectively. V is the volume of the solution (L) and W is the mass of dry sorbent used (g).

2.5. Effect of solution pH

The effect of solution pH was studied by agitating 0.30 g of OPTF and 200 mL of dye solution of dye concentration 100 mg/L using water-bath shaker at 30 °C. The experiment was conducted at different pH from 2 to 10. Agitation was provided for 195 min contact time which is sufficient to reach equilibrium with a constant agitation speed of 130 rpm. At equilibrium, the dye concentrations were measured by a double beam UV/vis spectrophotometer (Shimadzu, Model UV 1601, Japan) at 618 nm. The pH was adjusted by adding a few drops of diluted 0.1N NaOH or 0.1N HCl before each experiment. The pH was measured by using a pH meter (Ecoscan, EUTECH Instruments, Singapore).

2.6. Adsorption kinetics

For kinetic studies, 0.30 g of OPTF was contacted with 200 mL malachite green solutions of dye concentrations 25–300 mg/L using water-bath shaker at 30 °C and pH 5. The agitation speed was kept constant at 130 rpm. At predetermined intervals of time, solutions were analyzed for the final concentration of malachite green by a double beam UV/vis spectrophotometer (Shimadzu, Model UV 1601, Japan) at a wavelength of 618 nm, maximum absorbance.

3. Results and discussion

3.1. Characteristics of the adsorbent

Specific surface area (SSA) is the accessible area of adsorbent surface per unit mass of material. Because the surrounding phase can modify the surface area, each method used for measuring the surface area has its shortcomings and uncertainties. The interference by the surrounding phase is especially problematic for the Bruner-Emmet-Teller (BET) N_2 adsorption/desorption isotherm method because the entire surface is modified by vacuum treatment before N_2 adsorption. As an alternative to the BET method, the adsorption of dyes from aqueous solution has been used to determine the SSA of many substances such as layered silicate [31], sludge ash [32] and cotton [33]. Assuming that the OPTF surface is homogenous and completely covered by dye molecules, the SSA (m^2/g) of OPTF can then be related to the first layer adsorption density (Γ_m) as described in Eq. (2):

$$SSA = \Gamma_m N A \quad (2)$$

where N is the Avogadro's number (6.023×10^{23} molecules/mol) and A is the apparent surface area occupied by one MG molecule. The value of adsorption capacity is calculated as (shown in Section 3.4 below). Studies have shown that MG molecules are adsorbed in a flat orientation, so that the occupied surface area of one molecule of MG is196 $Å^2$ [34]. The SSA of OPTF calculated from Eq. (2) is 64.44 m^2/g.

FTIR spectrum (figure not shown) of OPTF shows distinct peaks at 3433.83 (O–H stretch), 2942.26 (C–H stretch), 2379.68 (N–H stretch), 1610.98 (NH_2 deformation), 1497.83 (Phenyl), 1458.01 (CH_2 deformation), 1384.03 (CH_3 deformation), 1272.83 (Si–C stretch), 1164.36 (C–N stretch), 1053.41 (C–O stretch), 772.6 cm^{-1} (CH_2 rocking) and 685.52 (C–S stretch). It is clear that the adsorbent displays a number of absorption peaks, reflecting the complex nature of the adsorbent.

Fig. 2 shows the SEM micrographs of OPTF samples before after dye adsorption. The OPTF exhibits a caves-like, uneven and rough surface morphology. The surface of dye-loaded adsorbent, however, clearly shows that the surface of OFTF is covered with a layer of dye.

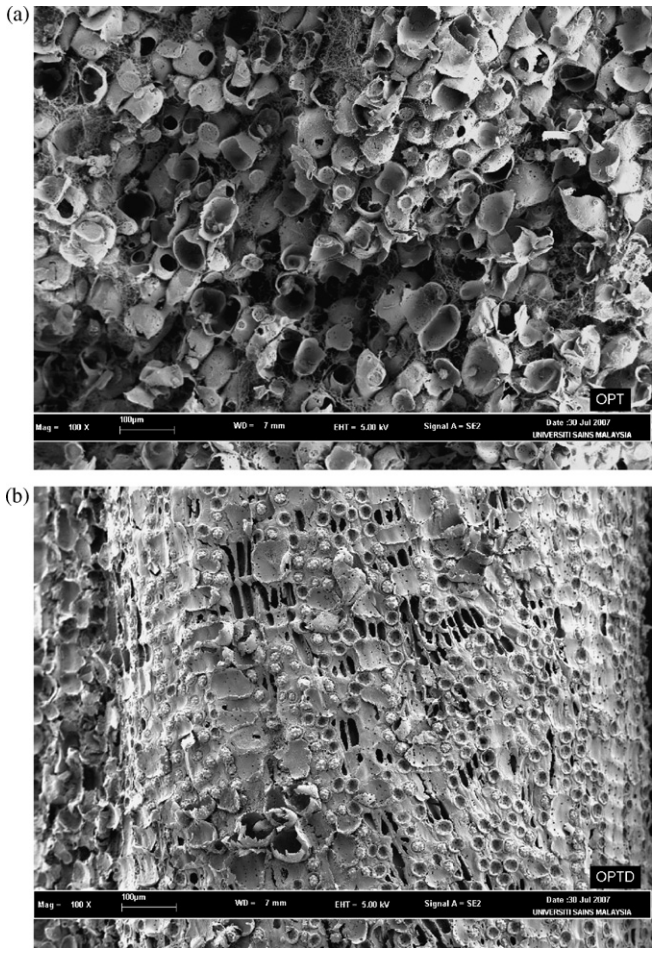

Fig. 2. SEM micrograph of OPTF particle (magnification, 100): (a) before dye sorption and (b) with dye adsorbed.

3.2. Effect of initial dye concentration and agitation time on dye adsorption

In order to study the effect of the initial concentration of MG in the solutions on the rate of adsorption on OPTF, the experiments were carried out at a fixed adsorbent dose (0.30 g) and at different initial dye concentrations of malachite green (25, 50, 100, 150, 200 and 300 mg/L) for different time intervals (10, 25, 45, 75, 105, 135, 165 and 195 min) at 30 °C. Fig. 3 shows the effect of the initial dye concentration on the adsorption. As the initial MG concentration increases from 25 to 300 mg/L the

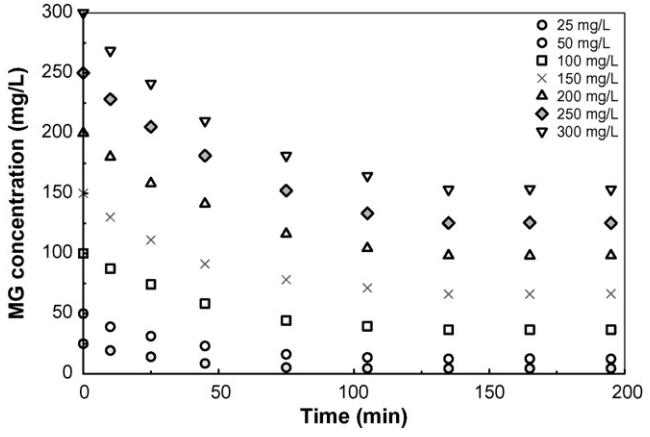

Fig. 3. Effect of initial concentration and contact time on malachite green adsorption (adsorbent dose = 0.30 g; temperature = 30 °C).

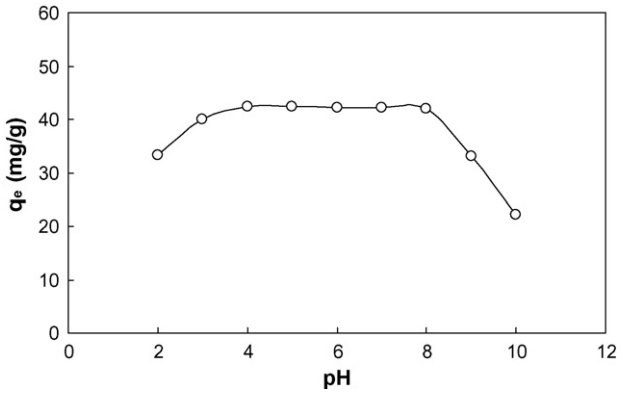

Fig. 4. Effect of pH on equilibrium uptake of MB (W = 0.30 g; V = 0.20 L; C_o = 100 mg/L).

equilibrium removal of MG decreases from 82 to 43%. It is also shown in Fig. 3 that the contact time needed for MG solutions with initial concentrations of 25–100 mg/L to reach equilibrium at 115 min. For MG solutions with initial concentrations of 150–300 mg/L, equilibrium time of 140 min was required. However, the experimental data were measured at 195 min to make sure that full equilibrium was attained.

3.3. Effect of pH on dye adsorption

The experiments were conducted at 100 mg/L initial dye concentration with 0.30 g adsorbent mass at 30 °C for 200 min equilibrium time. Fig. 4 shows the effect of pH on the adsorption of MG by OPTF. It can be seen that dye adsorption was unfavorable at pH < 4. The decrease in the adsorption with decrease in pH may be attributed to two reasons. As pH of the system decreased, the number of negatively charged adsorbent sites decreased and the number of positively charged surface sites increased, which did not favor the adsorption of positively charged dye cations due to electrostatic repulsion. Secondly lower adsorption of MG at acidic pH is due to the presence of excess H^+ ions competing with dye cations for the adsorption sites of OPTF [35]. This, however, did not explain the slight decrease of dye adsorption at higher pH values. There might be another mode of adsorption (ion exchange or chelatation for example) [35]. Similar result was reported for the adsorption on methylene on cedar sawdust and crushed brick [35].

3.4. Equilibrium isotherms

In this study, three isotherms were used for describing the experimental results, namely the Freundlich isotherm, the Langmuir isotherm, and the multilayer adsorption isotherm (MLA). The Freundlich isotherm is used for non-ideal adsorption on heterogeneous surfaces. The heterogeneity arises from the presence of different functional groups on the surface, and the various adsorbent–adsorbate interactions. The Freundlich isotherm is expressed by the following empirical equation [36]:

$$q_e = K_F C_e^{1/n} \tag{3}$$

where K_F is the Freundlich adsorption constant and $1/n$ is a measure of the adsorption intensity.

The derivation of the Langmuir isotherm assumes ideal monolayer adsorption on a homogenous surface. It is expressed by [37]:

$$q_e = \frac{q_m K_a C_e}{1 + K_a C_e} \tag{4}$$

where C_e is the equilibrium concentration (mg/L), q_e is the amount of dye adsorbed (mg/g), q_m is q_e for complete monolayer adsorption capacity (mg/g), and K_a is the equilibrium adsorption constant (L/mg).

If the adsorption takes place in a multilayer equilibrium on a homogenous surface, the total multilayer adsorption capacity (Γ, mg/g) can be expressed by the following equation [38]:

$$\Gamma = \frac{\Gamma_m K_1 C_e [1 - (K_2 C_e)^n]}{1 - K_2 C_e)[1 + (K_1 - K_2) C_e]} \tag{5}$$

where Γ_m is the monolayer adsorption capacity (mg/g), K_n is (L/mg) the equilibrium adsorption constant of the nth layer and C_e is the equilibrium MG concentration (mg/L). In the case of multilayer adsorption, the amount of MG adsorbed in a subsequent layer must be smaller than that in the previous layer. Therefore, the term $(K_2 C_e)^n \approx 0$, and Eq. (5) can be simplified to:

$$\Gamma = \frac{\Gamma_m K_1 C_e}{(1 - K_2 C_e)[1 + (K_1 - K_2) C_e]} \tag{6}$$

It can be seen that for ideal monolayer adsorption K_2 will have a value of zero, and Eq. (6) will be reduced to the monolayer Langmuir isotherm of Eq. (4).

Fig. 5 shows the fitted equilibrium data in Freundlich, Langmuir, and the multilayer adsorption (MLA) expressions. The fitting results, i.e. isotherm parameters and the coefficient of determination, R^2, are shown in Table 1. It can be seen in Fig. 5 that the MLA curve fits the data better than Freundlich and Langmuir models, this is also confirmed by the high value of R^2 in case of MLA (0.9990) compared to Freundlich (0.9928) and Langmuir (0.9575). This indicates that the adsorption of MG on OPTF takes place as a multilayer adsorption on a surface that is homogenous in adsorption affinity.

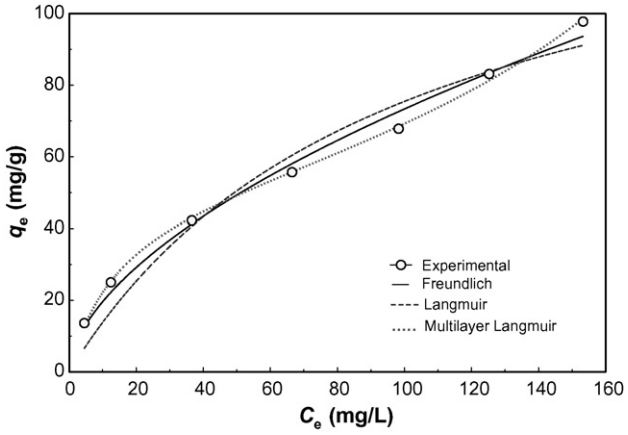

Fig. 5. Isotherm plots for MG adsorption on OTPF at 30 °C.

Table 1
Isotherm constants for MG adsorption on OPTF at 30 °C

Langmuir isotherm model			Freundlich isotherm model			Multilayer adsorption model			
q_m (mg/g)	K_a (L/mg)	R^2	K_F (mg/g) (L/mg)$^{1/n}$	n	R^2	Γ_m (mg/g)	K_1 (L/mg)	K_2 (L/mg)	R^2
149.35	0.01022	0.9575	5.248	1.746	0.9928	50.61	0.07103	0.003321	0.9990

3.5. Performance of OPTF

Table 2 compares the adsorption capacity of different types of adsorbents used for removal of MG [21,39–44]. The most important parameter to compare is the Langmuir q_m value since it is a measure of adsorption capacity of the adsorbent. The value of q_m in this study is larger than those in most of previous works. This suggests that MG could be easily adsorbed on OPTF.

3.6. Kinetic study

In order to investigate the kinetics of adsorption of MG on OPTF, the Lagergren pseudo-first-order model (Eq. (7)) [45], Ho's pseudo-second-order model (Eq. (8)) [46], and the Elovich model (Eq. (9)) [47] were used.

$$q = q_e(1 - e^{-k_1 t}) \quad (7)$$

$$q = \frac{q_e^2 k_2 t}{1 + q_e k_2 t} \quad (8)$$

$$q = \left(\frac{1}{\beta}\right) \ln(1 + \alpha\beta t) \quad (9)$$

where q_e is the amount of adsorbate adsorbed at equilibrium (mg/g), q is the amount of adsorbate adsorbed at time t (mg/g), k_1 is the rate constant of pseudo-first-order adsorption (min^{-1}), k_2 is the rate constant of pseudo-second-order adsorption (g/mg min), α is the initial adsorption rate (mg/g min), and β is the desorption constant (g/mg).

The fittings of the experimental kinetic results to the models are shown in Figs. 6–8, and the values of the estimated param-

Table 2
Comparison of adsorption capacities of various adsorbents for malachite green

Adsorbent	q_m (mg/g)	T (°C)	References
OPTF	149.35	30	This work
Arundo donax root carbon (ADRC)	8.70	30	[39]
Activated charcoal	0.179	30	[40]
Bentonite clay	7.72	35	[41]
Waste apricot	116.27	30	[42]
Activated carbon	149	25	[43]
Bagasse fly ash (BFA)	170.33	30 ± 1	[21]
Activated carbons commercial grade (ACC)	8.27	30 ± 1	[21]
Laboratory grade activated carbons (ACL)	42.18	30 ± 1	[21]
Commercially available powdered activated carbon	222.22	30 ± 1	[44]
Groundnut shell based powdered activated carbon	222.22	30 ± 1	[44]

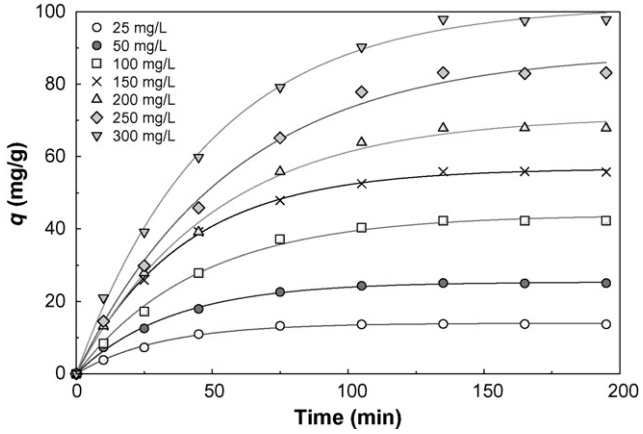

Fig. 6. The fitting of Lagergren's model for MG on OTPF for different initial concentrations at 30 °C.

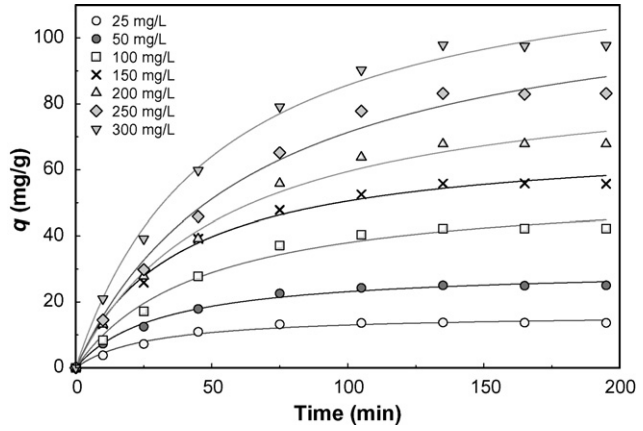

Fig. 7. The fitting of pseudo-second-order model for MG on OTPF for different initial concentrations at 30 °C.

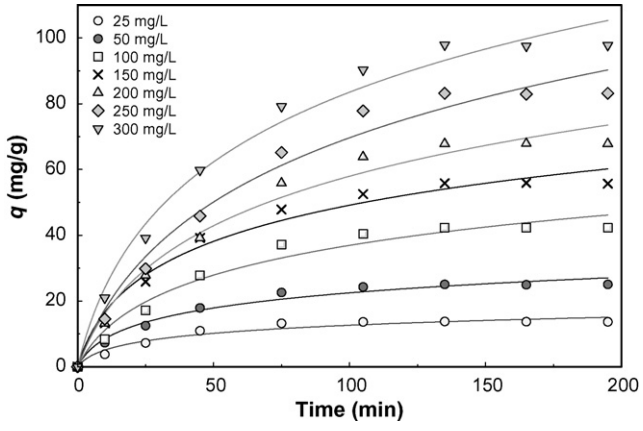

Fig. 8. The fitting of Elovich model for MG on OTPF for different initial concentrations at 30 °C.

Table 3
Kinetic models parameters for the adsorption of MG on OPTF at 30 °C and different initial MG concentrations (C_o, mg/L; q_e, mg/g; k_1, min^{-1}; k_2, g/mg min, α, mg/g min; and β, g/mg)

C_o	q_{exp}	Pseudo-first order			Pseudo-second order			Elovich equation		
		q_e	k_1	R^2	q_e	k_2	R^2	α	β	R^2
25	13.71	13.97	0.03239	0.9968	16.49	0.002256	0.9827	1.087	0.2703	0.9577
50	25.02	25.33	0.02864	0.9976	30.30	0.001062	0.9928	1.644	0.1420	0.9787
100	42.30	43.92	0.02233	0.9967	55.34	0.0003947	0.9870	1.662	0.06794	0.9724
150	55.81	56.70	0.02536	0.9992	69.46	0.0003845	0.9941	2.796	0.05787	0.9809
200	67.86	71.20	0.01966	0.9968	91.43	0.0002034	0.9910	2.260	0.03968	0.9815
250	83.09	89.04	0.01733	0.9958	117.72	0.0001306	0.9895	2.272	0.02917	0.9809
300	97.78	101.67	0.0203	0.9981	129.46	0.0001513	0.9938	3.442	0.02851	0.9853

eters are presented in Table 3. It was found that the fitting to Lagergren's pseudo-first-order model gives the highest values of R^2 (0.9958–0.9992) and predicts q_e more accurately than the other two models investigated. Therefore, Lagergren's model could be used for the prediction of the kinetics of adsorption of MG on OPTF. The initial rates of adsorption were calculated from Lagergren's model and the pseudo-second-order models from the equations:

$$h_{o,1} = k_1 q_e \tag{10}$$

$$h_{o,2} = k_2\, q_e^2 \tag{11}$$

and the results are plotted in Fig. 9. It was found that the initial rate of adsorption increases with increasing the initial MG concentration, which would be expected due to the increase in driving force at higher concentration. The anomaly of h_o at $C_o = 150$ mg/L is probably due to an experimental error in the measurement of q at the early stages of adsorption.

3.7. Sorption mechanism

In order to gain insight into the mechanisms and rate-controlling steps affecting the kinetics of adsorption, the kinetic experimental results were fitted to the Weber's intraparticle diffusion [48] and Boyd's film-diffusion [49] models.

The intraparticle-diffusion parameter, k_i (mg/g min$^{0.5}$) is defined by the following equation:

$$q = k_i t^{0.5} + c \tag{12}$$

where q is the amount of MG adsorbed (mg/g) at time t, k_i is intraparticle-diffusion constant (mg/g min$^{0.5}$), and c is the intercept. If the value of c is zero, then the rate of adsorption is controlled by intraparticle diffusion for the entire adsorption period. However, the plot of q against $t^{0.5}$ usually shows more than one linear portion, and if the slope of the first portion is not zero, then film (boundary layer) diffusion controls the adsorption rate at the beginning. Fig. 10 shows the intraparticle-diffusion plot of MG adsorption on OTPF at 30 °C. It is obvious that the plot is multilinear. In order to avoid subjective judgment in choosing the beginning and end of each linear region, the package Number Crunching Statistical Software package (NCSS) [50] was used to fit the data to the models by the method of piecewise linear regression, the regression results are presented in Table 4. It was found that for initial MG concentrations 25, 50,150, and 300 mg/L the rate of adsorption is initially controlled by film diffusion then changes to intraparticle-diffusion control after 55–71 min. On the other hand, for initial MG concentrations 200 and 250 mg/L the rate of adsorption is controlled by film diffusion from the beginning until equilibrium. Of course there is a possibility that just before equilibrium there may be

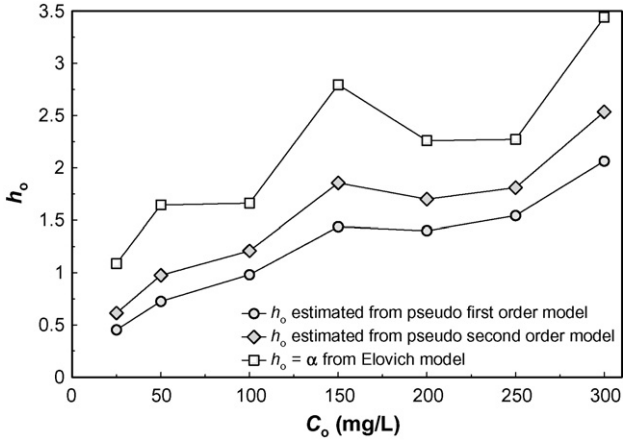

Fig. 9. The variation of the initial rate of adsorption with the initial MG concentration.

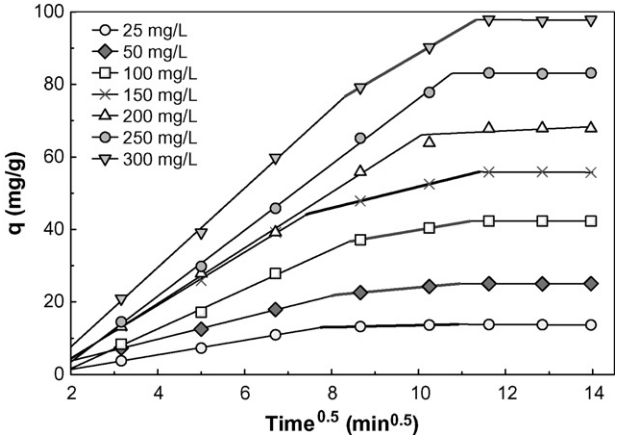

Fig. 10. Intraparticle-diffusion plot for the adsorption at 30 °C and different initial MG concentrations, the thick lines represent the intraparticle-diffusion periods.

Table 4
Diffusion coefficients for adsorption of MG on OTPF at 30 °C, and different initial concentrations (C_o, mg/L; c, mg/g; k_s, min^{-1}; D_i, cm^2/s)

C_o	$D_i \times 10^6$	c	k_i	Pore-diffusion period[a]
25	7.50	10.98	0.2605	60–119
50	6.59	13.27	1.0753	64–120
100	7.04	19.66	2.0201	71–125
150	6.55	22.42	2.9370	55–130
200	5.68	–	–	–
250	5.08	–	–	–
300	5.51	18.59	6.996	69–128

[a] Estimated from the second linear region according to the pore-diffusion model (min).

a short period in which the rate of adsorption is controlled by intraparticle diffusion, but the time intervals between the experimental points (30 min) does not allow the identification of this period with any certainty. It is also seen in Table 4 that the intraparticle-diffusion coefficient increases with increasing concentration of MG. This can be explained by examining the values of q at the start of intraparticle-diffusion control; the overall adsorption rate is controlled by intraparticle diffusion when the values of q are about 12, 20, 35, 45, and 72 mg/g for initial MG concentrations 25, 50,150, and 300 mg/L, respectively. The increasing values of surface loading increase the driving force for intraparticle diffusion.

The film-diffusion model of Boyd is expressed as:

$$F = 1 - \left(\frac{6}{\pi^2}\right)\exp(-Bt) \tag{13}$$

where F is the fractional attainment of equilibrium, at different times, t, and Bt is a function of F.

$$F = \frac{q_t}{q_e} \tag{14}$$

where q_t and q_e are the dye uptake (mg/g) at time t and at equilibrium, respectively.

Eq. (13) can be rearranged to

$$Bt = -0.4977 - \ln(1 - F) \tag{15}$$

Fig. 11 shows the Boyd plots of MG adsorption on OTPF at 30 °C. The plots are linear in the initial period of adsorption and do not pass through the origin but have intercept values close to −0.4977, indicating that external mass transfer is the rate limiting process in the beginning of adsorption. It should be noted that the values of Bt become less reliable as equilibrium is approached. For example, if a small experimental error (1%) changes the value of F from 0.95 to 0.9595, the value of Bt changes by 8.4% from 2.498 to 2.708. The same effect if even more exaggerated at higher values of F. Therefore, the Boyd plots cannot be used to predict the time at which film-diffusion control ends if the transition happens to be close to equilibrium. The slopes obtained from piecewise linear regressions (B) were used to calculate the effective diffusion coefficient, D_i (cm^2/s) from the equation:

$$B = \frac{\pi^2 D_i}{r^2} \tag{16}$$

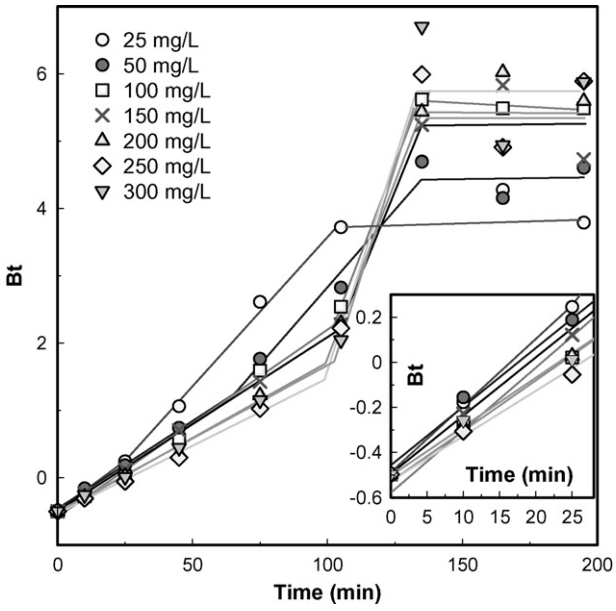

Fig. 11. Boyd plots for MG adsorption on OTPF at 30 °C and different initial MG concentrations.

where r is the radius of the adsorbent particle assuming spherical shape. The values of D_i in Table 4 show that D_i decreases with the increase in C_o. The domination of film diffusion for initial MG concentrations 200 and 250 mg/L takes place at relatively low values of D_i, 5.68×10^{-6} and 5.08×10^{-6} cm^2/s, respectively.

4. Conclusions

Oil palm trunk fibre, an agricultural solid waste, was successfully utilized as a low-cost alternative adsorbent for the removal of hazardous dye like MG. The equilibrium adsorption data were analyzed by the Freundlich isotherm, the Langmuir isotherm, and the multilayer adsorption isotherm. The results indicate that the multilayer adsorption isotherm fits the data better than the other two models. The monolayer adsorption capacity of OPTF based on Langmuir isotherm was found to be 149.35 mg/g at 30 °C. It was found that the Lagergren's model could be used for the prediction of the kinetics of adsorption of MG on OPTF. The overall rate of dye uptake was found to be controlled by external mass transfer at the beginning of adsorption, then for some initial MG concentrations the rate-control changed to intraparticle diffusion at a later stage, but for initial MG concentrations 200 and 250 mg/L no evidence was found of intraparticle diffusion at any period of adsorption.

References

[1] S.D. Khattri, M.K. Singh, Colour removal from dye wastewater using sugar cane dust as an adsorbent, Adsorpt. Sci. Technol. 17 (4) (1999) 269–282.
[2] L. Papinutti, N. Mouso, F. Forchiassin, Removal and degradation of the fungicide dye malachite green from aqueous solution using the system wheat bran—*Fomes sclerodermeus*, Enzyme Microb. Technol. 39 (2006) 848–853.
[3] C.F. Chang, C.H. Yang, Y.O. Shu, T.I. Chen, M.S. Shu, I.C. Liao, Effects of temperature, salinity and chemical drugs on the in vitro propagation of the Dinoflagellate parasite, *Amylodinium ocellatum*, Asian Fish Soc. (2001) P31.

[4] R.A. Schnick, The impetus to register new therapeutants for aquaculture, Prog. Fish Cult. 50 (1988) 190–196.
[5] I.A. Rahman, B. Saad, S. Shaidan, E.S. Sya Rizal, Adsorption characteristics of malachite green on activated carbon derived from rice husks produced by chemical–thermal process, Bioresour. Technol. 96 (2005) 1578–1583.
[6] S. Srivastava, R. Sinha, D. Roy, Toxicological effects of malachite green, Aquat. Toxicol. 66 (3) (2004) 319–329.
[7] R.F.P. Nogueira, M.R.A. Silva, A.G. Trovó, Influence of the iron source on the solar photo-Fenton degradation of different classes of organic compounds, Sol. Energy 79 (2005) 384–392.
[8] K. Wu, Y. Xie, J. Zhao, H. Hidaka, Photo-Fenton degradation of a dye under visible light irradiation, J. Mol. Catal. A Chem. 144 (1999) 77–84.
[9] C. Hachem, F. Bocquillon, O. Zahraa, M. Bouchy, Decolourization of textile industry wastewater by the photocatalytic degradation process, Dyes Pigments 49 (2001) 117–125.
[10] H. Kominami, H. Kumamoto, Y. Kera, B. Ohtani, Photocatalytic decolorization and mineralization of malachite green in an aqueous suspension of titanium(IV) oxide nano-particles under aerated conditions: correlation between some physical properties and their photocatalytic activity, J. Photochem. Photobiol. A Chem. 160 (2003) 99–104.
[11] F. Sayılkan, M. Asiltürk, P. Tatar, N. Kiraz, E. Arpaç, H. Sayılkan, Photocatalytic performance of Sn-doped TiO_2 nanostructured mono and double layer thin films for Malachite Green dye degradation under UV and vis-lights, J. Hazard. Mater. 144 (2007) 140–146.
[12] C.A. Başar, Y. Önal, T. Kılıçer, D. Eren, Adsorptions of high concentration malachite green by two activated carbons having different porous structures, J. Hazard. Mater. B127 (2005) 73–80.
[13] S. Rajgopal, T. Karthikeyan, B.G. Prakash Kumar, L.R. Miranda, Utilization of fluidized bed reactor for the production of adsorbents in removal of malachite green, Chem. Eng. J. 116 (2006) 211–217.
[14] B.H. Hameed, A.T.M. Din, A.L. Ahmad, Adsorption of methylene blue onto bamboo-based activated carbon: kinetics and equilibrium studies, J. Hazard. Mater. 141 (2007) 819–825.
[15] I.A.W. Tan, B.H. Hameed, A.L. Ahmad, Equilibrium and kinetic studies on basic dye adsorption by oil palm fibre activated carbon, Chem. Eng. J. 127 (2007) 111–119.
[16] B.H. Hameed, A.L. Ahmad, K.N.A. Latiff, Adsorption of basic dye (methylene blue) onto activated carbon prepared from rattan sawdust, Dyes Pigments 75 (2007) 143–149.
[17] I.A.W. Tan, A.L. Ahmad, B.H. Hameed, Optimization of preparation conditions for activated carbons from coconut husk using response surface methodology, Chem. Eng. J. 137 (2008) 462–470.
[18] B.H. Hameed, F.B.M. Daud, Adsorption studies of basic dye on activated carbon derived from agricultural waste: *Hevea brasiliensis* seed coat, Chem. Eng. J. 139 (2008) 48–55.
[19] A. Mittal, L. Krishnan, V.K. Gupta, Removal and recovery of malachite green from wastewater using an agricultural waste material, de-oiled soya, Sep. Purif. Technol. 43 (2005) 125–133.
[20] V.K. Garg, R. Rakesh Kumar, Gupta, Removal of malachite green dye from aqueous solution by adsorption using agro-industry waste: a case study of *Prosopis cineraria*, Dyes Pigments 62 (2004) 1–10.
[21] I.D. Mall, V.C. Srivastava, N.K. Agarwal, I.M. Mishra, Adsorptive removal of malachite green dye from aqueous solution by bagasse fly ash and activated carbon-kinetic study and equilibrium isotherm analyses, Colloids Surf. A Physicochem. Eng. Aspects 264 (2005) 17–28.
[22] A. Mittal, Adsorption kinetics of removal of a toxic dye, Malachite Green, from wastewater by using hen feathers, J. Hazard. Mater. B133 (2006) 196–202.
[23] P. Janoš, V. Šmídová, Effects of surfactants on the adsorptive removal of basic dyes from water using an organomineral sorbent–iron humate, J. Colloid Interface Sci. 291 (2005) 19–27.
[24] R. Gong, Y. Jin, F. Chen, J. Chen, Z. Liu, Enhanced malachite green removal from aqueous solution by citric acid modified rice straw, J. Hazard. Mater. 137 (2006) 865–870.
[25] S. Sumathi, S.P. Chai, A.R. Mohamed, Utilization of oil palm as a source of renewable energy in Malaysia, Renew Sustain Energy Rev., in press (doi:10.1016/j.rser.2007.06.006).
[26] M.Z.B. Hussein, M.B.B. Abdul Rahman, A.H.J. Yahaya, T.Y.Y.H.N. Ahmad, Oil palm trunk as a raw material for activated carbon production, J. Porous Mater. 8 (2001) 327–334.
[27] K.O. Lim, The future energy potential of replanting wasted in Malaysia, Renewable Energy 8 (1986) 76–85.
[28] K.O. Lim, K.S. Lim, Carbonisation of oil palm trunks at moderate temperatures, Bioresour. Technol. 40 (1992) 215–219.
[29] K.O. Lim, F.H. Ahmaddin, S.M. Vizhi, A note on the conversion of oil-palm trunks to glucose via acid hydrolysis, Bioresour. Technol. 59 (1997) 33–35.
[30] R. Sun, J. Tomkinson, Fractional separation and physico-chemical analysis of lignins from the black liquor of oil palm trunk fibre pulping, Sep. Purif. Technol. 24 (2001) 529–539.
[31] R.A. Shelden, W.R. Caseri, U.W. Suter, Ion exchange on muscovite mica with ultrahigh specific surface area, J. Colloid Interface Sci. 157 (1993) 318–327.
[32] C.H. Weng, Adsorption characteristics of new coccine dye on to sludge ash, Adsorpt. Sci. Technol. 20 (2002) 669–681.
[33] C. Kaewprasit, E. Hequet, N. Abidi, J.P. Gourlot, Application of methylene blue adsorption to cotton fiber specific surface area measurement. Part I. Methodology, J. Cotton Sci. 2 (1998) 164–173.
[34] C.H. Giles, R.B. McKay, Adsorption of cationic (basic) dyes by fixed yeast cells, J. Bacteriol. 89 (1965) 390–397.
[35] O. Hamdaoui, Batch study of liquid-phase adsorption of methylene blue using cedar sawdust and crushed brick, J. Hazard. Mater. B135 (2006) 264–273.
[36] H.M.F. Freundlich, Uber die adsorption in Losungen, Z. Phys. Chem. 57 (1906) 385.
[37] I. Langmuir, Constitution and fundamental properties of solids and liquids. I. Solids, J. Am. Chem. Soc. 38 (11) (1916) 2221.
[38] J. Wang, C.P. Huang, H.E. Allen, D.K. Cha, D.W. Kim, Adsorption characteristics of dye onto sludge particulates, J. Colloid Interface Sci. 208 (1998) 518–528.
[39] J. Zhang, et al., Adsorption of malachite green from aqueous solution onto carbon prepared from Arundo donax root, J. Hazard. Mater. 150 (2008) 774–782.
[40] M.J. Iqbal, M.N. Ashiq, Adsorption of dyes from aqueous solutions on activated charcoal, J. Hazard. Mater. B139 (2007) 57–66.
[41] S.S. Tahir, N. Rauf, Removal of a cationic dye from aqueous solutions by adsorption onto bentonite clay, Chemosphere 63 (2006) 1842–1848.
[42] C.A. Başar, Applicability of the various adsorption models of three dyes adsorption onto activated carbon prepared apricot, J. Hazard. Mater. B135 (2006) 232–241.
[43] Y. Önal, C. Akmil-Başar, C. Sarıcı-Ö zdemir, Investigation kinetics mechanisms of adsorption malachite green onto activated carbon, J. Hazard. Mater. 146 (2007) 194–203.
[44] R. Malik, D.S. Ramteke, S.R. Wate, Adsorption of malachite green on groundnut shell waste based powdered activated carbon, Waste Manage. 27 (2007) 1129–1138.
[45] S. Lagergren, Zur theorie der sogenannten adsorption geloster stoffe. 591. Kungliga Svenska Vetenskapsakademiens, Handlingar 24 (4) (1898) 1–39.
[46] Y.S. Ho, Adsorption of heavy metals from waste streams by peat, Ph.D. Thesis, University of Birmingham, Birmingham, U.K., 1995.
[47] C. Aharoni, D.L. Sparks, S. Levinson, I. Ravina, Kinetics of soil chemical reactions: relationships between empirical equations and diffusion models, Soil Sci. Soc. Am. J. 55 (1991) 1307–1312.
[48] W.J. Weber Jr., J.C. Morris, Kinetics of adsorption on carbon from solution, J. Sanitary Eng. Div. Proceed. Am. Soc. Civil Eng. 89 (1963) 31–59.
[49] G.E. Boyd, A.W. Adamson, L.S. Myers Jr., The exchange adsorption of ions from aqueous solutions by organic zeolites, II: kinetics, J. Am. Chem. Soc. 69 (1947) 2836–2848.
[50] J. Hintze, NCSS, PASS, and GESS. NCSS, Kaysville, Utah, 2006.